Quarterly Journal of the Royal Meteorological Society *Q. J. R. Meteorol. Soc.* 143: 670–677, January 2017 B DOI:10.1002/qj.2955

RMetS
Royal Meteorological Society

Oscillations in Prandtl slope flow started from rest

E. Fedorovich[a]* and A. Shapiro[a,b]

[a]*School of Meteorology, University of Oklahoma, Norman, OK, USA*
[b]*Center for Analysis and Prediction of Storms, University of Oklahoma, Norman, OK, USA*

*Correspondence to: E. Fedorovich, School of Meteorology, University of Oklahoma, 120 David L. Boren Blvd, NWC/SoM, Norman, OK 73072, USA. E-mail: fedorovich@ou.edu

We study oscillations that develop in flows along a uniform planar slope in an initially resting stratified fluid as a result of sudden application of a surface buoyancy flux. After an oscillatory adjustment (transition), the fluid reaches another steady state that corresponds to a stationary slope flow. The analysis is focused on the temporal evolution of the integral momentum and buoyancy structure in the laminar Prandtl-type slope flow. The main questions addressed are related to physical conditions leading to emerging of the *en masse* oscillations in the transitioning slope flow, the frequency of these oscillations, and features of their temporal evolution. The persistence of oscillations in Prandtl-type slope flows is found to be associated, somewhat paradoxically, with the fast temporal decay of the surface stress oscillations in the process of the stress approaching a constant value. This relatively rapid evolution of the surface stress progressively weakens damping of the integral momentum and buoyancy oscillations. Extensions of the analyses to the Prandtl slope flow driven by the surface buoyancy and to the turbulent slope flows are proposed and discussed.

Key Words: buoyancy; damping; oscillator; Prandtl model; surface stress

Received 26 July 2016; Revised 21 October 2016; Accepted 27 October 2016; Published online in Wiley Online Library 27 December 2016

1. Introduction

Anabatic (upslope) and katabatic (downslope) winds are two common boundary-layer-type flows observed in the atmosphere above sloping terrain. From the fluid-dynamical standpoint, such slope winds are buoyantly (or convectively) driven motions of a stratified fluid along heated (anabatic flow) or cooled (katabatic flow) sloping surfaces. Despite recent progress in the conceptual understanding of the slope flows in their idealized or prototypic forms, that is, assuming an infinite planar slope with a spatially uniform surface thermal forcing and linear thermal stratification of the ambient fluid (see review in Fedorovich and Shapiro (2009)), some outstanding questions remain regarding various aspects of the physical behaviour of such flows. Of particular interest in this respect are oscillatory slope flow regimes associated with transitions between steady states of the flow under the effect of changing surface thermal forcing.

In this study we analytically investigate oscillations that develop in laminar slope flows along a uniform planar slope in a stably stratified atmosphere as the result of a sudden application of the surface buoyancy flux. The stratified fluid, which fills the space above the slope, is initially at rest. After an oscillatory adjustment, the fluid reaches another steady state that corresponds either to a stationary katabatic flow (in the case of a negative surface buoyancy flux) or to a stationary anabatic flow (in the case of a positive surface buoyancy flux).

An early milestone in the description of katabatic/anabatic flows was the Prandtl (1942) analytical model of the laminar natural-convection flow of a viscous stably stratified fluid along a uniformly cooled or heated sloping planar surface. Flow in Prandtl's one-dimensional model has a boundary-layer character (low-level jet topped by weak reversed flow). The model describes a slope flow in mechanical and thermodynamical equilibrium, where the along-slope advection of environmental potential temperature balances the buoyancy diffusion, and the along-slope component of buoyancy balances diffusion of along-slope momentum. All other terms in the equations of motion and buoyancy balance are identically zero. Observations suggest that, with appropriately tuned mixing parameters, this simple model provides an overall realistic description of the vertical structure of slope flows (e.g. Defant, 1949; Tyson, 1968; Papadopoulos *et al.*, 1997; Oerlemans, 1998).

Analytical solutions for unsteady Prandtl-like slope flows starting from rest were considered in several studies. Gutman and Malbakhov (1964) extended the unsteady Prandtl-flow model to include the Coriolis force, though Egger (1985) noted several unphysical aspects of that solution; see also Stiperski *et al.* (2007) and Shapiro and Fedorovich (2008). In a study of wind oscillations in katabatic flows, McNider (1982) solved the layer-averaged Prandtl equations with a highly idealized parametrization of the surface drag that was simply set proportional to the wind speed integrated over the slope-normal coordinate. Grisogono (2003) suggested that the assumed constancy of the eddy viscosity in the original Prandtl model produced near-surface wind gradients that were generally too weak and obtained an unsteady approximate solution of the Prandtl equations for a prescribed slowly varying (in slope-normal coordinate) eddy viscosity. Mo (2013) extended the McNider (1982) study of oscillations in katabatic flows by

including a Newtonian cooling term in the layer-averaged thermal energy equation.

Schumann (1990) used large-eddy simulation (LES) to investigate the developing turbulent anabatic boundary layer along a uniformly heated inclined plate immersed in a stably stratified fluid. In that study, transient momentum and temperature solutions underwent persistent oscillations with a frequency close to $N\sin\alpha$, where N is the Brunt–Väisälä (or buoyancy) frequency of the ambient fluid and α is the slope angle. In order to expedite a transition of the oscillatory solutions to the steady flow regime, Schumann (1990) forced damping of the oscillations by applying a specially designed relaxation algorithm. The employed numerical set-up permitted comparison of mean steady-state solutions with predictions of the Prandtl model, which indicated that for small- and moderate-angle slope flows, results of the Prandtl theory were supported fairly well by the numerical data, apart from structural differences in the mean-flow profile shapes.

A closer look at the oscillations in turbulent slope flows developing from rest was taken in a direct numerical simulation (DNS) study by Fedorovich and Shapiro (2009), who found that turbulent fluctuations of velocity and buoyancy in the near-wall regions of the flows were superimposed with persistent quasi-periodic oscillations which had a frequency close to the natural buoyancy frequency $N\sin\alpha$. These persistent oscillations were apparent far beyond the thermal and dynamic turbulent boundary layers developing along the slope and showed very little (if any) tendency to decay with time. Oscillatory flow patterns similar to the pattern observed in Fedorovich and Shapiro (2009) had been previously described by Shapiro and Fedorovich (2006) in their study of laminar natural convection flow along a wall with a temporally periodic surface thermal forcing. In the case of slope flow in Fedorovich and Shapiro (2009), however, there was no temporal variability in the surface forcing. Instead, the oscillatory motion was a result of an internal negative feedback mechanism acting in the stratified fluid system that was adapting to the new steady state. Such oscillations, analogous to the oscillations encountered by Schumann (1990), were also observed in the katabatic wind studies of Monti *et al.* (2002) and Princevac *et al.* (2008), where the frequency $N\sin\alpha$ was, apparently erroneously, attributed to internal gravity waves that arrive normal to the slope – rather than associating it with *en masse* flow oscillations (see Chemel *et al.*, 2009, p. 191).

In the present study, the oscillatory behaviour of laminar slope flows is investigated using nonstationary versions of the Prandtl (1942) model equations first derived and discussed by Defant (1949). Solutions of the Defant problem for the slope-flow case with time-periodic surface buoyancy forcing were recently obtained by Zardi and Serafin (2015), whose temporally evolving profiles of velocity and buoyancy turned out to be similar to the profiles from the aforementioned study of Shapiro and Fedorovich (2006), with direct correspondence between the profiles for the special case of flow along a vertical wall. The present study, however, is focused on the temporal evolution of the integral momentum and buoyancy structure of the slope flow started from rest by application of a time-constant surface buoyancy flux. The main questions to be addressed are related to the nature of the *en masse* oscillations in a slope flow transitioning between two steady states, the frequency of these oscillations, and features of their temporal evolution.

The governing equations of slope-flow dynamics, and their reduction to the Defant (1949) and Prandtl (1942) model equations are considered in section 2. In section 3, general solutions of the nonstationary equations for the integral momentum and buoyancy are obtained for a fluid that is initially at rest and eventually reaches the Prandtl (1942) equilibrium flow state after an oscillatory transition. The temporal evolution of the flow variables and other parameters is presented and analysed in section 4. Extensions of the results to related slope-flow types are presented and discussed in section 5.

2. Governing equations

We employ the Boussinesq equations of three-dimensional fluid motion in a right-hand Cartesian (x, y, z) coordinate system following an infinite planar slope tilted at angle α relative to the horizontal plane (Fedorovich and Shapiro, 2009). The x-axis is directed upslope, the y-axis is directed cross-slope, and the z-axis is directed normal to the slope. With the Coriolis force neglected, the equations of motion are

$$\frac{\partial u}{\partial t}+u\frac{\partial u}{\partial x}+v\frac{\partial u}{\partial y}+w\frac{\partial u}{\partial z} = -\frac{\partial \pi}{\partial x}+b\sin\alpha+\nu\left(\frac{\partial^2 u}{\partial x^2}+\frac{\partial^2 u}{\partial y^2}+\frac{\partial^2 u}{\partial z^2}\right), \quad (1)$$

$$\frac{\partial v}{\partial t}+u\frac{\partial v}{\partial x}+v\frac{\partial v}{\partial y}+w\frac{\partial v}{\partial z} = -\frac{\partial \pi}{\partial y}+\nu\left(\frac{\partial^2 v}{\partial x^2}+\frac{\partial^2 v}{\partial y^2}+\frac{\partial^2 v}{\partial z^2}\right), \quad (2)$$

$$\frac{\partial w}{\partial t}+u\frac{\partial w}{\partial x}+v\frac{\partial w}{\partial y}+w\frac{\partial w}{\partial z} = -\frac{\partial \pi}{\partial z}+b\cos\alpha+\nu\left(\frac{\partial^2 w}{\partial x^2}+\frac{\partial^2 w}{\partial y^2}+\frac{\partial^2 w}{\partial z^2}\right). \quad (3)$$

The thermal energy equation is formulated in terms of the buoyancy b as

$$\frac{\partial b}{\partial t}+u\frac{\partial b}{\partial x}+v\frac{\partial b}{\partial y}+w\frac{\partial b}{\partial z} = -N^2(u\sin\alpha+w\cos\alpha)+\nu_h\left(\frac{\partial^2 b}{\partial x^2}+\frac{\partial^2 b}{\partial y^2}+\frac{\partial^2 b}{\partial z^2}\right). \quad (4)$$

The mass conservation is given by the continuity equation for an incompressible fluid:

$$\frac{\partial u}{\partial x}+\frac{\partial v}{\partial y}+\frac{\partial w}{\partial z}=0. \quad (5)$$

In the above equations, u, v, and w are, respectively, the x, y, and z velocity components, ν is the kinematic viscosity, and ν_h is the thermal diffusivity. The normalized pressure perturbation is defined through $\pi=\{p-p_e(z')\}/\rho_r$, where $p_e(z')$ is the environmental pressure, z' is the true vertical coordinate which is directed opposite to the gravity acceleration vector, and $\rho_r=\text{const}$ is a reference density value. Buoyancy $b=\beta\theta$ is expressed in terms of the potential temperature perturbation $\theta=\Theta-\Theta_e(z')$, where Θ is potential temperature, $\Theta_e(z')$ is the environmental potential temperature, $\beta=g/\Theta_r$ is the buoyancy parameter, $\Theta_r=\text{const}$ is the constant reference potential temperature value, and g is the gravity acceleration magnitude. The vertical gradient of the environmental potential temperature, $\gamma=\mathrm{d}\Theta_e/\mathrm{d}z'$, is assumed to be constant, which implies also constancy of the environmental Brunt–Väisälä (or buoyancy) frequency $N=(\beta\gamma)^{1/2}$.

With the assumed flow homogeneity in the x and y directions, and $w=0$ on the slope, the incompressibility condition yields $w(x,y,z,t)=0$. Assuming additionally no cross-slope motion ($v=0$), the governing equations may be reduced to

$$\frac{\partial u}{\partial t}=b\sin\alpha+\nu\frac{\partial^2 u}{\partial z^2}, \quad (1a)$$

$$0=-\frac{\partial \pi}{\partial z}+b\cos\alpha, \quad (3a)$$

$$\frac{\partial b}{\partial t}=-N^2u\sin\alpha+\nu_h\frac{\partial^2 b}{\partial z^2}. \quad (4a)$$

The coupled Eqs (1a) and (4a) correspond to Defant's (1949) nonstationary Prandtl slope-flow case and were used in Zardi and Serafin (2015) to analytically study slope flows driven by time-periodic surface thermal perturbations. The Prandtl (1942) model equations,

$$0 = b\sin\alpha + \nu\frac{\partial^2 u}{\partial z^2}, \tag{1b}$$

$$0 = -N^2 u\sin\alpha + \nu_h\frac{\partial^2 b}{\partial z^2}, \tag{4b}$$

result from the further reduction of the governing equations by assuming the steady state. In Prandtl (1942), the solutions of Eqs (1b) and (4b) were obtained with a prescribed value of the surface buoyancy $b_s = b\text{—}_{z=0} = \text{const}$. Solutions of Eqs (1b) and (4b) for the case of a prescribed surface buoyancy flux, $-\nu_h\frac{\partial b}{\partial z}\big|_{z=0} = B_s = \text{const}$, are considered in Fedorovich and Shapiro (2009).

In the following section, vertically (over z) integrated Eqs (1a) and (4a) are derived and analysed for a special case of $\nu = \nu_h$ (i.e. for Prandtl number, $\mathrm{Pr} = \nu/\nu_h$, of unity). These equations are applied to investigate the evolution of the vertically integrated momentum and buoyancy fields in a slope flow developing from rest and forced by a specified surface buoyancy flux $B_s = \text{const}$.

3. Analysis of the integral momentum and buoyancy equations

We first normalize the independent and dependent variables in Eqs (1a) and (4a) using the scales $\nu^{1/2}N^{-1/2}\sin^{-1/2}\alpha$ for length, $\nu^{-1/2}N^{-3/2}B_s$ for velocity, $\nu^{-1/2}N^{-1/2}B_s$ for buoyancy, and $N^{-1}\sin^{-1}\alpha$ for time. The first three scales are similar to the ones that have been used in Fedorovich and Shapiro (2009) to normalize the Prandtl (1942) model equations for the case of slope flow driven by the buoyancy flux. In terms of the normalized quantities, Eqs (1a) and (4a) appear as

$$\frac{\partial u}{\partial t} = b + \frac{\partial^2 u}{\partial z^2}, \tag{1c}$$

$$\frac{\partial b}{\partial t} = -u + \frac{\partial^2 b}{\partial z^2}, \tag{4c}$$

where we keep the same notation for the normalized variables as for their dimensional counterparts. The normalized Eqs (1c) and (4c) complemented with the normalized surface condition for the buoyancy flux, $-\frac{\partial b}{\partial z}\big|_{z=0} = 1$, are identical to the normalized momentum and buoyancy balance equations employed in Shapiro and Fedorovich (2004) to describe a non-stationary convectively driven flow along a vertical wall.

Integrating Eqs (1c) and (4c) over z from 0 to ∞ noting that both dimensionless momentum and buoyancy fluxes ($-\partial u/\partial z$ and $-\partial b/\partial z$, respectively) vanish at $z \to \infty$, we obtain the integral budget of the x-component of momentum,

$$\frac{\mathrm{d}I_u}{\mathrm{d}t} = I_b - \tau, \tag{6}$$

and the integral budget of buoyancy

$$\frac{\mathrm{d}I_b}{\mathrm{d}t} = -I_u + 1, \tag{7}$$

where $I_u = \int_0^\infty u\,\mathrm{d}z$ and $I_b = \int_0^\infty b\,\mathrm{d}z$ are the normalized velocity and buoyancy integrals, respectively, and $\tau = \frac{\partial u}{\partial z}\big|_{z=0}$ is the dimensionless surface shear stress.

Differentiating Eqs (6) and (7) with respect to t and combining terms, we come up with two oscillator equations, one for the integral momentum,

$$\frac{\mathrm{d}^2 I_u}{\mathrm{d}t^2} + I_u = 1 - \frac{\mathrm{d}\tau}{\mathrm{d}t}, \tag{8}$$

and another for the integral buoyancy,

$$\frac{\mathrm{d}^2 I_b}{\mathrm{d}t^2} + I_b = \tau. \tag{9}$$

Apart from being written in dimensionless form, Eqs (8) and (9) are equivalent to the oscillatory slope-flow equations in Schumann (1990), who derived these equations for the turbulent flow fields averaged over slope-parallel planes. The resulting oscillator equations (16) and (17) in Schumann (1990) have exactly the same form as Eqs (8) and (9). Schumann (1990) suggested that these relationships describe oscillations of I_u and I_b with a weak damping maintained by the surface stress (friction) τ. However, as will be shown below, the damping may also be zero even if the surface stress is present.

Solutions of Eqs (8) and (9) for I_u and I_b that satisfy initial conditions of no motion and no buoyancy ($I_u = 0$ and $I_b = 0$ at $t = 0$) are

$$I_u(t) = 1 - \cos t - \int_0^t \tau(t')\cos(t - t')\mathrm{d}t', \tag{10}$$

$$I_b(t) = \sin t + \int_0^t \tau(t')\sin(t - t')\mathrm{d}t'. \tag{11}$$

Although Eqs (10) and (11) contain oscillatory terms, one cannot conclude that the resulting solutions are oscillatory without knowing how τ behaves. In the special case of no surface friction ($\tau = 0$), the integrals on the right-hand sides of Eqs (10) and (11) vanish. In this case, the slope flow perpetually oscillates with a normalized natural frequency of 1, and the momentum and buoyancy oscillations are shifted in phase by $\pi/2$ with respect to each other.

Let us consider, as another option, the case where the surface stress τ attains a steady state after a finite time t^*. For times $t > t^*$, Eqs (10) and (11) can be solved as

$$I_u(t) = I_u(t^*) + \cos t^* - \cos t - \tau\sin(t - t^*), \tag{12}$$

$$I_b(t) = I_b(t^*) + \sin t - \sin t^* + \tau\{1 - \cos(t - t^*)\}. \tag{13}$$

We thus see that the constant-stress solutions of Eqs (8) and (9) for $t > t^*$ are of an undamped oscillator. Remarkably, the constant surface stress will not provide any damping, and oscillations of I_u and I_b will persist indefinitely long.

Now consider a situation where the surface stress is proportional to the velocity integral, i.e. $\tau = kI_u$, where k is a constant non-negative parameter. Such a drag-type proportionality assumption is analogous to the one adopted by McNider (1982). In this case, Eq. (8) can be rewritten as

$$\frac{\mathrm{d}^2 I_u}{\mathrm{d}t^2} + k\frac{\mathrm{d}I_u}{\mathrm{d}t} + I_u = 1, \tag{14}$$

A particular solution of Eq. (14) is $I_u = 1$. Homogeneous solutions are of the form $I_u \sim \mathrm{e}^{mt}$ provided m satisfies $m^2 + km + 1 = 0$. We solve for m to get

$$m = (-k \pm \sqrt{k^2 - 4})/2, \tag{15}$$

Further evaluation of the solution depends on the value of the discriminant k^2-4. In the case of $0 \le k^2 < 4$, the homogeneous solution for I_u has the form of an underdamped oscillator:

$$I_u = \mathrm{e}^{-\frac{kt}{2}}\left\{a\cos\left(\frac{t}{2}\sqrt{4-k^2}\right)+b\sin\left(\frac{t}{2}\sqrt{4-k^2}\right)\right\}. \quad (16)$$

The particular solution of Eq. (14) that satisfies the initial condition of no motion and no buoyancy (from Eq. (6), $I_b = \mathrm{d}I_u/\mathrm{d}t = 0$ initially) is therefore

$$I_u = 1-\mathrm{e}^{-\frac{kt}{2}}\left\{\cos\left(\frac{t}{2}\sqrt{4-k^2}\right)+\frac{k}{\sqrt{4-k^2}}\sin\left(\frac{t}{2}\sqrt{4-k^2}\right)\right\}. \quad (17)$$

Applying Eq. (17) in Eq. (6), we obtain the corresponding solution for I_b in the form:

$$I_b = k-\mathrm{e}^{-\frac{kt}{2}}\left\{k\cos\left(\frac{t}{2}\sqrt{4-k^2}\right)-\frac{2-k^2}{\sqrt{4-k^2}}\sin\left(\frac{t}{2}\sqrt{4-k^2}\right)\right\}. \quad (18)$$

In the case of $k=0$, the relationships Eqs (17) and (18) reduce to the undamped oscillator solutions with normalized frequency of unity:

$$I_u = 1-\cos t, \quad I_b = \sin t. \quad (19)$$

This solution also follows from Eqs (10) and (11) for the case of zero surface stress. As follows from Eqs (17) and (18), the factor k plays three main roles in the underdamped oscillator. First, it controls the damping efficiency of the oscillator, so that oscillations die out faster with larger k. Second, it modulates the frequency of oscillations by shifting it toward lower values compared to the normalized natural frequency of 1. Finally, it regulates the offset between the equilibrium levels of I_u and I_b, with $k=1$ being the value at which these levels are the same. The special case $\tau = kI_u$ with $k=2$ corresponds to the so-called critically damped oscillator. When $k \ge 2$, oscillations are no longer possible. In this so-called overdamped case, the solutions approach their equilibrium values without oscillations.

Figure 1 presents an overview of I_u, I_b and τ behaviour for different values of k in the solutions Eqs (17) and (18) for the underdamped oscillator with $\tau = kI_u$. The case of $k=0$ (plot (a)) corresponds to an undamped oscillator with zero surface stress, and I_u and I_b that harmonically vary in time with a dimensionless period 2π (corresponding to the normalized angular frequency 1) and dimensionless amplitude 1. The case of $k=0.1$ (plot (b)) corresponds to a weakly damped oscillator with the amplitudes of the I_u and I_b oscillations decaying with time as $\mathrm{e}^{-0.05t}$. Due to the weak damping, one cannot visually trace in the plot the lowering of the oscillation frequency to 0.999 and the period increase to 6.29. However, changes in both the parameters start becoming noticeable in the plot for $k=0.5$ ((c); the case of moderate damping), where the amplitudes decay with time as $\mathrm{e}^{-0.25t}$, the normalized frequency drops to 0.968, and the period rises to 6.49. With strong damping ((d); case of $k=1$), the resulting amplitude decay ($\propto \mathrm{e}^{-0.5t}$), as well as the oscillation frequency decrease (down to 0.866; with period increase to 7.26), become apparent.

One may reinterpret the behaviour of the McNider (1982) oscillator with different degrees of damping in terms of dimensional flow variables. For typical slope-flow conditions represented by $N = 10^{-2}$ s^{-1}, $\nu = 1$ m^2 s^{-1}, $B_s = 10^{-2}$ m^2 s^{-3}, and $\alpha = 30^\circ$, we obtain a length scale of 14.1 m, velocity scale of 10 m s^{-1}, buoyancy scale of 0.1 m s^{-2}, and time scale of 200 s. This time scale corresponds to a dimensional natural frequency of 5×10^{-3} s^{-1} and a natural oscillation period roughly equal to 1256 s, both of which appear to be within their observed ranges for slope flows in nature (Chemel *et al.*, 2009). The dimensional damping factor (drag coefficient) k_d, expressed as k multiplied by the ratio of the velocity and length scales, is equal to 0.71 k s^{-1}. Now one can estimate the dimensional rate of oscillation decay in terms of the e-folding time with different damping factors. Noticing from Eq. (16) that the dimensionless e-folding time is given by $t_e = 2/k$ and renormalizing t_e accordingly, we obtain the following estimates of the dimensional e-folding time t_{ed} for different values of damping factor: $t_{ed} = 4000$ s for the weakly damped oscillator ($k=0.1$), $t_{ed} = 800$ s for the moderately damped oscillator ($k=0.5$), and $t_{ed} = 400$ s for the strongly damped oscillator ($k=0.5$). All flow variables shown in Figure 1 may be rescaled to atmospheric dimensions using the length, velocity and buoyancy scales specified above. The rescaling of τ indicates, in particular, that in order to get realistic values of surface stress using the McNider (1982) model, the value of k needs to be much smaller than 0.1.

4. Oscillatory solutions for flow integrals and surface stress

The analyses presented in section 3 indicate that knowledge of the relationship between the surface stress and integral momentum is key to understanding the oscillatory behaviour of the Prandtl flow developing from rest. One may independently diagnose this relationship from the non-stationary solutions for u and b using results of Shapiro and Fedorovich (2004), where Eqs (1c) and (4c) were solved semi-analytically, with u and b obtained in the form of integrals that need to be evaluated numerically. These integrals (using notation adopted in the current article) are

$$u(z,t) = \frac{z}{2\pi}\int_0^t \frac{\sin(t-t')}{(t-t')^{3/2}}\int_0^{t'}\frac{\sin t''}{t''^{3/2}}\exp\left(-\frac{z^2}{4t''}\right)\mathrm{d}t''\mathrm{d}t', \quad (20)$$

and

$$b(z,t) = \frac{z}{2\pi}\int_0^t \frac{\sin(t-t')}{(t-t')^{3/2}}\int_0^{t'}\frac{\cos t''}{t''^{3/2}}\exp\left(-\frac{z^2}{4t''}\right)\mathrm{d}t''\mathrm{d}t'. \quad (21)$$

Using Eq. (20) to evaluate $\frac{\partial u}{\partial z}\big|_{z=0}$, one obtains the surface stress

$$\tau(t) = \left.\frac{\partial u}{\partial z}\right|_{z=0} = \frac{1}{2\pi}\int_0^t \frac{\sin(t-t')}{(t-t')^{3/2}}\int_0^{t'}\frac{\sin t''}{t''^{3/2}}\mathrm{d}t''\mathrm{d}t'. \quad (22)$$

For the vertically integrated u, Eq. (20) provides

$$I_u(t) = \int_0^\infty u\,\mathrm{d}z = \frac{1}{\pi}\int_0^t \frac{\sin(t-t')}{(t-t')^{3/2}}\int_0^{t'}\frac{\sin t''}{t''^{1/2}}\mathrm{d}t''\mathrm{d}t'. \quad (23)$$

Finally, the vertically integrated b is obtained using Eq. (21) as

$$I_b(t) = \int_0^\infty b\,\mathrm{d}z = \frac{1}{\pi}\int_0^t \frac{\sin(t-t')}{(t-t')^{3/2}}\int_0^{t'}\frac{\cos t''}{t''^{1/2}}\mathrm{d}t''\mathrm{d}t'. \quad (24)$$

The solutions Eqs (22)–(24) are plotted in Figure 2. The behaviour of the solutions for I_u and I_b at small times $t \lesssim 4\pi$ reveals strong initial damping that progressively weakens with time. At $t \gtrsim 8\pi$, the damping is virtually undetectable. On the other hand, the surface stress τ, which initially shows noticeable fluctuations, rapidly approaches a constant value of unity. This relatively fast decrease of the amplitude of τ oscillations – as compared to the decay of the I_u and I_b oscillations – happens in accordance with Eq. (22), which contains a factor of $(t'')^{-3/2}$ in the second integral on the right-hand side, while analogous terms in Eqs (23) and (24) behave as $(t'')^{-1/2}$. The I_u and I_b integrals oscillate in antiphase, as determined by the $\sin t''$ term in Eq. (23) versus the $\cos t''$ term in Eq. (24), while τ oscillations are in phase with I_u as Eqs (22) and (23) both contain $\sin t''$ under the integrals on the right-hand sides. As τ rapidly becomes

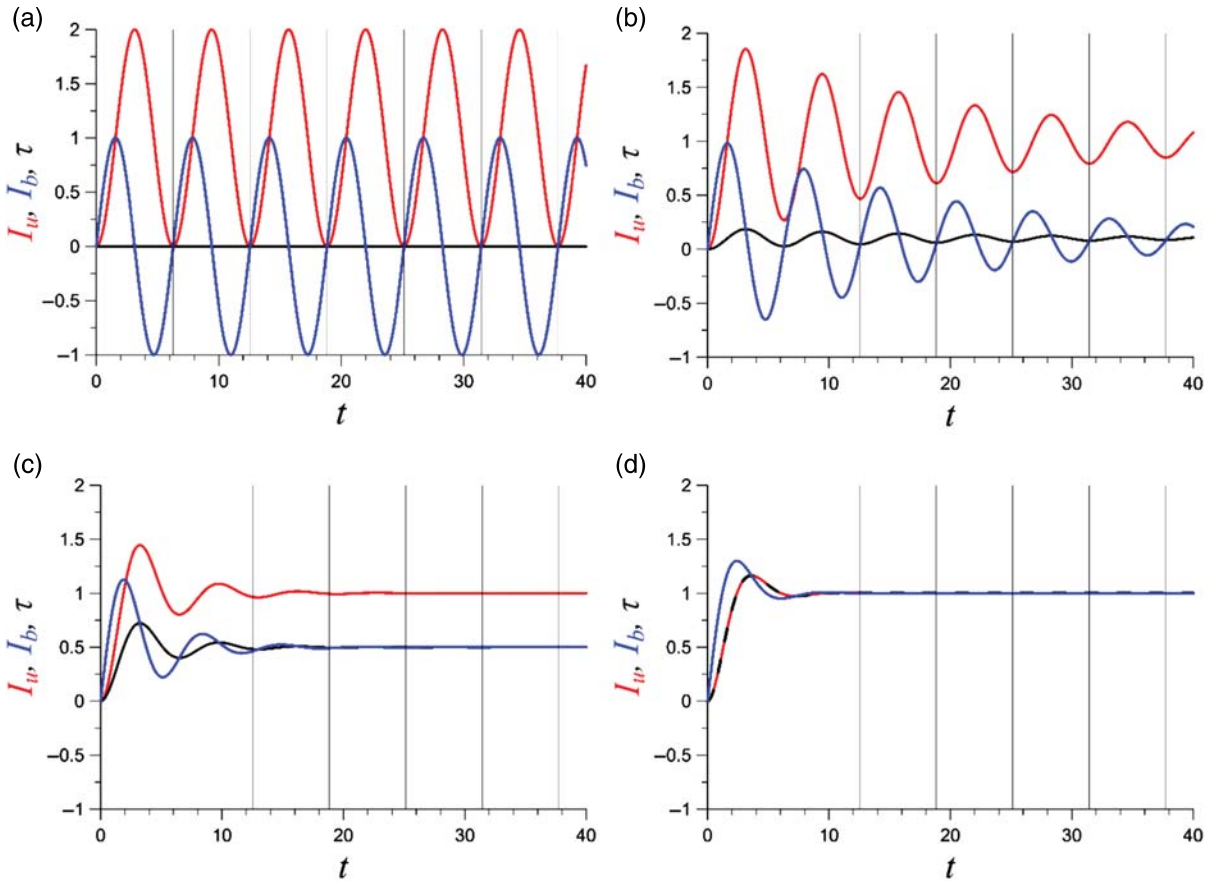

Figure 1. Evolution of the integral momentum I_u (red lines) and buoyancy I_b (blue lines) in the regime of underdamped oscillations with surface stress $\tau = kI_u$ (black lines) for different values of damping parameter k: (a) $k = 0$, (b) $k = 0.1$, (c) $k = 0.5$, and (d) $k = 1$. Thin vertical lines indicate 2π time intervals corresponding to the normalized natural frequency of 1.

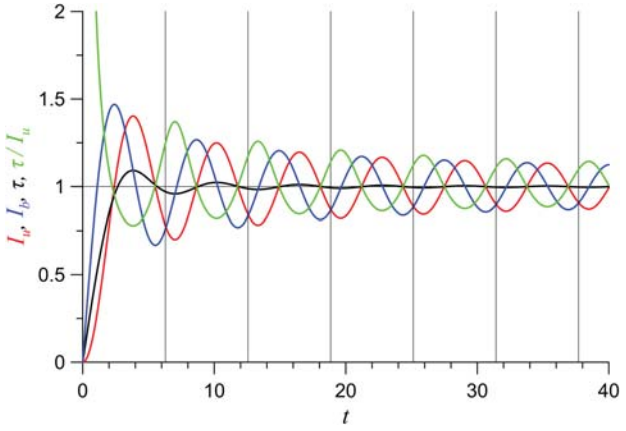

Figure 2. Dimensionless integral momentum I_u (red line), integral buoyancy I_b (blue line), and surface stress τ (black line) evaluated, respectively, from Eqs (23), (24) and (22) as functions of dimensionless time t. Green line illustrates the evolution of the τ to I_u ratio (the counterpart of the damping parameter k in the underdamped oscillator theory). Thin vertical lines indicate 2π time intervals corresponding to the normalized natural frequency of 1.

practically constant, its damping effect on the integrals I_u and I_b significantly diminishes, and the decay of the I_u and I_b oscillations progressively weakens. In accordance with Eqs (12) and (13), the damping would be non-existent in the case of τ being exactly constant. Despite the fact that oscillations eventually die out while the flow reaches a steady state at $t \to \infty$ (Shapiro and Fedorovich, 2004), the flow conversion to such steady state in terms of $I_u \to 1$ and $I_b \to 1$ happens very slowly in comparison to the rate of τ converging to 1. Thus, the persistence of *en masse* oscillations in Prandtl-type slope flows appears to be associated with the fast decay of the surface stress oscillations which promotes the attenuation of damping of the integral momentum and buoyancy oscillations.

Figure 2 also depicts the temporal behaviour of the τ/I_u ratio. The strong variability of τ/I_u with time indicates that the assumption of constancy of this ratio adopted by McNider (1982) is actually not valid in the considered flow case. Values of the damping (drag) coefficient $k = \tau/I_u$ are very large during the early stage of the transition (at $t \lesssim 2\pi/3$), which points to a very strong damping at this stage, and then fluctuate around 1 with the magnitude of fluctuations decaying very slowly while remaining in antiphase with I_u.

The relation between the surface stress τ and the momentum integral I_u is additionally illustrated in Figure 3. The coupling between these two flow parameters is strong at the initial stages of the flow development (small t), when values of both variables are smaller than 1. Actually, for very small times t and given $0 \le t'' \le t' \le t$, one may approximate $\sin(t - t')$ by $t - t'$ and $\sin t''$ by t'', which then turn Eqs (22) and (23) into

$$\tau(t) = \frac{1}{\pi}\int_0^t \frac{t'^{\,1/2}}{(t-t')^{1/2}}\,\mathrm{d}t' = p\,t, \tag{25}$$

$$I_u(t) = \frac{2}{3\pi}\int_0^t \frac{t'^{\,3/2}}{(t-t')^{1/2}}\,\mathrm{d}t' = q\,t^2, \tag{26}$$

where p and q are the definite integrals $p \equiv \frac{1}{\pi}\int_0^1 \frac{\mu^{1/2}}{(1-\mu)^{1/2}}\,\mathrm{d}\mu$ and $q \equiv \frac{2}{3\pi}\int_0^1 \frac{\mu^{3/2}}{(1-\mu)^{1/2}}\,\mathrm{d}\mu$, where μ is a dummy variable of integration. These integrals can be explicitly evaluated as $p = 1/2$ and $q = 1/4$, which provides $\tau = \sqrt{I_u}$ for small t. This behaviour is evident in Figure 3.

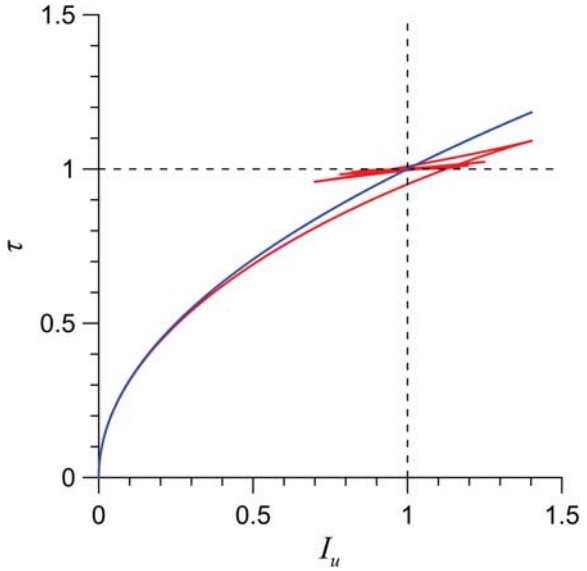

Figure 3. Red line: dimensionless surface stress τ from Eq. (22) plotted against dimensionless integral momentum I_u from Eq. (23). Blue line: $\tau = {I_u}^{1/2}$.

Later on, during the oscillatory flow phase, the correlation between the stress and momentum integral gradually becomes weaker as the stress becomes essentially constant, while the momentum integral continues to oscillate. This weakening correlation is evidenced by the changes in orientation of the individual pieces of the red line that progressively become directed more parallel to the I_u axis with each new oscillation.

5. Extension to related slope-flow cases

In the previous section, we obtained solutions of the non-stationary equations for integral momentum and buoyancy for a fluid above a sloping surface that is initially at rest and eventually reaches the Prandtl (1942) equilibrium flow state in the process of an oscillatory transition. Solutions were obtained for the flow driven by the surface buoyancy flux. It was found that quasi-persistent oscillations of the flow in terms of its periodic integral momentum and buoyancy fluctuations are associated with the relatively fast convergence of the surface stress to a near-constant value. This results in an attenuation of the damping effect of surface friction on the oscillations.

Similar behaviour is found in the Prandtl-type slope flow started from rest and driven by a time-constant surface buoyancy. Based on analyses of Shapiro and Fedorovich (2004) and Fedorovich and Shapiro (2009), the nonstationary Prandtl flow equations for this forcing type may be normalized with appropriate scales to obtain dimensionless equations of the same form as Eqs (1c) and (4c), but subject to a different surface boundary condition for the dimensionless buoyancy: $b|_{z=0} = 1$.

Integrating Eqs (1c) and (4c) over z from 0 to ∞ noting that both $\partial u/\partial z$ and $\partial b/\partial z$ vanish at $z \to \infty$, we obtain the integral budget of the x-component of momentum,

$$\frac{\mathrm{d}I_u}{\mathrm{d}t} = I_b - \tau, \tag{6a}$$

and the integral budget of buoyancy

$$\frac{\mathrm{d}I_b}{\mathrm{d}t} = -I_u + \beta, \tag{7a}$$

where $I_u = \int_0^\infty u\,\mathrm{d}z$, $I_b = \int_0^\infty b\,\mathrm{d}z$ and $\tau = \frac{\partial u}{\partial z}\big|_{z=0}$ have been defined previously, and $\beta = -\frac{\partial b}{\partial z}\big|_{z=0}$ is the dimensionless surface buoyancy flux.

Differentiating Eqs (6a) and (7a) with respect to t and combining terms, we come up with the oscillator equations

$$\frac{\mathrm{d}^2 I_u}{\mathrm{d}t^2} + I_u = \beta - \frac{\mathrm{d}\tau}{\mathrm{d}t}, \tag{8a}$$

$$\frac{\mathrm{d}^2 I_b}{\mathrm{d}t^2} + I_b = \tau + \frac{\mathrm{d}\beta}{\mathrm{d}t}. \tag{9a}$$

The solutions of Eqs (8a) and (9a) for I_u and I_b that satisfy initial conditions of no motion and no buoyancy ($I_u = 0$ and $I_b = 0$ at $t = 0$) are

$$I_u(t) = -\int_0^t \tau(t')\cos(t-t')\mathrm{d}t' + \int_0^t \beta(t')\sin(t-t')\mathrm{d}t', \tag{10a}$$

$$I_b(t) = \int_0^t \tau(t')\sin(t-t')\mathrm{d}t' + \int_0^t \beta(t')\cos(t-t')\mathrm{d}t'. \tag{11a}$$

Let us consider a case of steady τ and β, and examine the implications of such shear stress and buoyancy flux constancy for solutions of Eqs (8a) and (9a). For times $t > t^*$, where t^* is any finite post-transition time, I_u and I_b in Eqs (10a) and (11a) can be evaluated as

$$I_u(t) = I_u(t^*) - \tau\sin(t-t^*) + \beta\{1-\cos(t-t^*)\}, \tag{12a}$$

$$I_b(t) = I_b(t^*) + \tau\{1-\cos(t-t^*)\} + \beta\sin(t-t^*). \tag{13a}$$

We thus see that the constant-stress and constant-flux solutions of Eqs (8a) and (9a) for $t > t^*$ are again of an undamped oscillator type. Consequently, under conditions of constancy of the surface stress and surface buoyancy flux there will be no damping in the fluid system, and oscillations of I_u and I_b will go on indefinitely.

Now one needs to determine how τ and β actually change with time in the case of the surface buoyancy condition. To do this, we use the corresponding solutions of Eqs (6a) and (7a) with $b|_{z=0} = 1$ from Shapiro and Fedorovich (2004):

$$u(z,t) = \frac{z}{2\sqrt{\pi}}\int_0^t \frac{\sin t'}{t'^{3/2}}\exp\left(-\frac{z^2}{4t'}\right)\mathrm{d}t', \tag{20a}$$

$$b(z,t) = \frac{z}{2\sqrt{\pi}}\int_0^t \frac{\cos t'}{t'^{3/2}}\exp\left(-\frac{z^2}{4t'}\right)\mathrm{d}t'. \tag{21a}$$

Evaluating $\frac{\partial u}{\partial z}\big|_{z=0}$ from Eq. (20a) and $\frac{\partial b}{\partial z}\big|_{z=0}$ from Eq. (21a), one obtains the following expressions for the normalized surface stress and buoyancy flux:

$$\tau(t) = \left.\frac{\partial u}{\partial z}\right|_{z=0} = \frac{1}{2\sqrt{\pi}}\int_0^t \frac{\sin t'}{t'^{3/2}}\,\mathrm{d}t', \tag{22a}$$

$$\beta(t) = -\left.\frac{\partial b}{\partial z}\right|_{z=0} = -\frac{1}{2\sqrt{\pi}}\int_0^t \frac{\cos t'}{t'^{3/2}}\,\mathrm{d}t'. \tag{27}$$

On the other hand, for the vertically integrated u and b, Eqs (20a) and (21a) provide

$$I_u(t) = \int_0^\infty u\,\mathrm{d}z = \frac{1}{\sqrt{\pi}}\int_0^t \frac{\sin t'}{t'^{3/2}}\,\mathrm{d}t'. \tag{23a}$$

$$I_b(t) = \int_0^\infty b\,\mathrm{d}z = \frac{1}{\sqrt{\pi}}\int_0^t \frac{\cos t'}{t'^{3/2}}\,\mathrm{d}t'. \tag{24a}$$

Comparing the rates of decay with time of the integrands in Eqs (22a) and (27) to the analogous terms in (23a) and (24a), we conclude that, like in the case of the slope flow with the

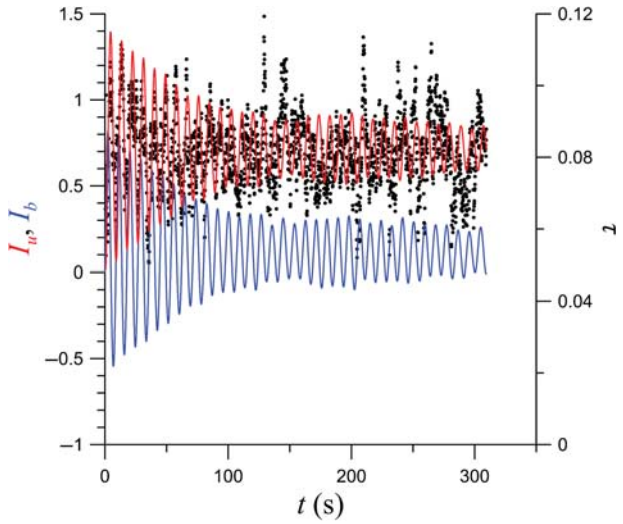

Figure 4. Time evolution of the dimensional surface stress τ (in $m^2\,s^{-2}$; black dots) in relation to dimensional momentum and buoyancy integrals I_u (in $m^2\,s^{-1}$; red line) and I_b (in $m^2\,s^{-2}$; blue line) in the turbulent anabatic flow driven by a constant surface buoyancy flux.

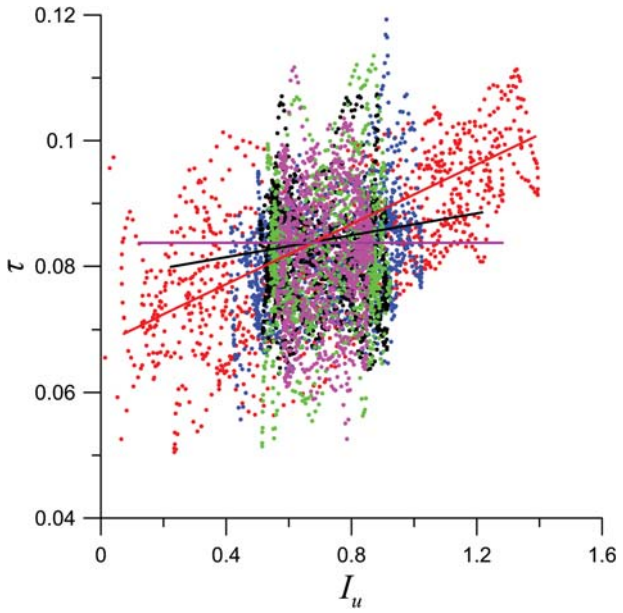

Figure 5. Scatter plot of dimensional surface stress τ (in $m^2\,s^{-2}$) versus dimensional momentum integral I_u (in $m^2\,s^{-1}$) corresponding to the time series depicted in Figure 4. Different point colours illustrate a changing relation between τ and I_u at different stages of the flow evolution: $t < 66$ s (red); $66\,\text{s} \le t < 112$ s (blue); $112\,\text{s} \le t < 178$ s (black); $178\,\text{s} \le t < 244$ s (green); and $244\,\text{s} \le t < 310$ s (magenta). Red line shows a linear fit of $\tau(I_u)$ for $t < 66$ s, black line for $112\,\text{s} \le t < 178$ s, and magenta line for $244\,\text{s} \le t < 310$ s.

surface buoyancy flux boundary condition, periodic fluctuations of the integral momentum and buoyancy in the Prandtl-type flow driven by the surface buoyancy are expected to decay with time very slowly due to variations in the surface damping rapidly decreasing with t.

The conducted analyses of the role of the surface stress in promoting/damping integral oscillations in slope flows of Prandtl type may be extended to the turbulent analogues of the Prandtl flow studied in detail numerically in Fedorovich and Shapiro (2009). In that study, numerically simulated turbulent katabatic and anabatic flows exhibited persistent oscillatory behaviour after being started from rest. Like in the case of the Prandtl flow, the frequency of the ensuing oscillations was close to $N \sin\alpha$. With respect to the basic features of the mean structure (obtained by averaging over the planes parallel to the slope and over time), the simulated turbulent slope flows also appeared qualitatively similar to their corresponding laminar counterparts. With the Reynolds decomposition and averaging applied only over the planes parallel to the slope, the normalized governing equations of the turbulent slope flow integrated in the slope-normal direction acquire the same forms as the nonstationary Prandtl-flow Eqs (6) and (7), but with I_u and I_b signifying the normalized integrals of the mean velocity and buoyancy, respectively, and τ retaining the meaning of the dimensionless surface shear stress. This equivalence of integral forms of laminar Prandtl flow and its turbulent counterpart was demonstrated in Schumann (1990).

One may revisit numerical simulations from Fedorovich and Shapiro (2009) to investigate, in connection with results from the present study, the damping effect of the surface stress on the integral oscillations in a turbulent slope flow started from rest by application of the surface buoyancy flux. The surface stress and flow integrals were evaluated from the output of direct numerical simulation of an anabatic flow along a slope of $\alpha = \pi/4$, with $\nu = \nu_h = 10^{-4}$ $m^2\,s^{-1}$, $N = 1$ s^{-1}, and driven by a surface buoyancy flux of $B_s = 0.5$ $m^2\,s^{-3}$. The time evolution of the dimensional momentum and buoyancy integrals in this flow, and the corresponding surface stress, is illustrated in Figure 4.

Like in the case of the laminar Prandtl flow (see Figure 2), one can trace a close correlation between oscillations of τ and I_u at the earlier stages of transition which are evidenced by black dots closely following the red line for $t \lesssim 100$ s. This correlation is associated with the relatively strong damping of both I_u and I_b clearly seen in the plot. With time increasing, however, the behaviour of τ becomes more random and its correlation with I_u is essentially lost, although τ values in average remain close to a constant of about 0.08 $m^2\,s^{-2}$. Such overall constancy of the surface stress allows us to speculate, by analogy with the laminar Prandtl-flow oscillator, that the originally systematic surface damping transforms into a random damping forcing uncorrelated with the momentum integral.

This random damping is overall rather ineffective compared to the correlated damping at the earlier stages of transition, so the pace of decay of oscillations of the turbulent flow integrals decreases. The only principal difference compared to the laminar flow case is the noisiness of the τ data which is apparently a result of the turbulent character of the flow and limited averaging domain size.

This noisiness of the surface stress data in the case of turbulent Prandtl flow to a great extent obscures the correlation between τ and I_u additionally illustrated in Figure 5 (it may be considered a counterpart of Figure 3). One may clearly see, however, that the overall tendency of the τ versus I_u change with time points to the weakening correlation between the surface stress and the flow integral in the course of transition. At sufficiently large times (magenta points and line in Figure 5), the average τ remains essentially constant and does not depend on I_u. We thus infer that the progressive weakening of damping of *en masse* flow oscillations is apparently also a feature of a turbulent Prandtl flow started from rest.

Acknowledgements

Support from the National Science Foundation (USA) through grants ATM-0622745 and AGS-1359698 is gratefully acknowledged. We thank the anonymous referees for their helpful comments.

References

Chemel C, Staquet C, Largeron Y. 2009. Generation of internal gravity waves by a katabatic wind in an idealized Alpine valley. *Meteorol. Atmos. Phys.* **103**: 187–194.

Defant F. 1949. Zur Theorie der Hangwinde, nebst Bemerkungen zur Theorie der Berg- und Talwinde. *Arch. Meteorol. Geophys. Bioklim. A* **1**: 421–450.

Egger J. 1985. Slope winds and the axisymmetric circulation over Antarctica. *J. Atmos. Sci.* **42**: 1859–1867.

Fedorovich E, Shapiro A. 2009. Structure of numerically simulated katabatic and anabatic flows along steep slopes. *Acta Geophys.* **57**: 981–1010.

Grisogono B. 2003. Post-onset behaviour of the pure katabatic flow. *Boundary-Layer Meteorol.* **107**: 157–175.

Gutman LN, Malbakhov VM. 1964. On the theory of katabatic winds of Antarctic. *Meteorol. Issled.* **9**: 150–155 (in Russian).

McNider RT. 1982. A note on velocity fluctuations in drainage flows. *J. Atmos. Sci.* **39**: 1658–1660.

Mo R. 2013. On adding thermodynamic damping mechanisms to refine two classical models of katabatic winds. *J. Atmos. Sci.* **70**: 2325–2334.

Monti P, Fernando HJS, Princevac M, Chan WC, Kowalewski TA, Pardyjak ER. 2002. Observations of flow and turbulence in the nocturnal boundary layer over a slope. *J. Atmos. Sci.* **59**: 2513–2534.

Oerlemans J. 1998. The atmospheric boundary layer over melting glaciers. In *Clear and Cloudy Boundary Layers*, Holtslag AAM, Duynkerke PG. (eds.): 129–153. Royal Netherlands Academy of Arts and Sciences: Amsterdam.

Papadopoulos KH, Helmis CG, Soilemes AT, Kalogiros J, Papageorgas PG, Asimakopoulos DN. 1997. The structure of katabatic flows down a simple slope. *Q. J. R. Meteorol. Soc.* **123**: 1581–1601.

Prandtl L. 1942. *Führer durch die Strömungslehre*. Vieweg und Sohn: Braunschweig, Germany.

Princevac M, Hunt JCR, Fernando HJS. 2008. Quasi-steady katabatic winds on slopes in wide valleys: Hydraulic theory and observations. *J. Atmos. Sci.* **65**: 627–643.

Schumann U. 1990. Large-eddy simulation of the up-slope boundary layer. *Q. J. R. Meteorol. Soc.* **116**: 637–670.

Shapiro A, Fedorovich E. 2004. Unsteady convectively driven flow along a vertical plate immersed in a stably stratified fluid. *J. Fluid Mech.* **498**: 333–352.

Shapiro A, Fedorovich E. 2006. Natural convection in a stably stratified fluid along vertical plates and cylinders with temporally-periodic surface temperature variations. *J. Fluid Mech.* **546**: 295–311.

Shapiro A, Fedorovich E. 2008. Coriolis effects in homogeneous and inhomogeneous katabatic flows. *Q. J. R. Meteorol. Soc.* **134**: 353–370.

Stiperski I, Kavčič I, Grisogono B, Durran DR. 2007. Including Coriolis effects in the Prandtl model for katabatic flow. *Q. J. R. Meteorol. Soc.* **133**: 101–106.

Tyson PD. 1968. Velocity fluctuations in the mountain wind. *J. Atmos. Sci.* **25**: 381–384.

Zardi D, Serafin S. 2015. An analytic solution for time-periodic thermally driven slope flows. *Q. J. R. Meteorol. Soc.* **141**: 1968–1974.

